

Original Article

Preoperative Prediction of Ductal Carcinoma *in situ* Underestimation of the Breast using Dynamic Contrast Enhanced and Diffusion-weighted Imaging

Mina Park, Eun-Kyung Kim, Min Jung Kim, Hee Jung Moon

Department of Radiology and Research Institute of Radiological Science, Severance Hospital, Yonsei University, College of Medicine, Seoul, Korea

Objective: To investigate roles of dynamic contrast enhanced magnetic resonance (DCE MR) and diffusion-weighted (DW) imaging in preoperative prediction of underestimation of ductal carcinoma in situ (DCIS) ≥ 2 cm on US guided core needle biopsy.

Materials and Methods: Twenty two patients with DCIS on US-guided 14 gauge core needle biopsy were included. Patients were divided into a group with and without DCIS underestimation based on histopathology. MR images including DCE and DW imaging were obtained with a 3.0-T MR. The lesion type (mass or non-mass), enhancement pattern, peak enhancement, and apparent diffusion coefficient (ADC) values of proven malignant masses were generated using software of CADstream and compared between two groups using Fisher's exact test and Mann Whitney test.

Results: Eight patients were in the group with underestimation and 14 patients were in the group without underestimation. The lesion type and enhancement pattern were not different between two groups (P values = 1.000 and 0.613, respectively). The median peak enhancement of lesions with underestimation was 159.5%, higher than 133.5% of those without underestimation, but not significant (P value = 0.413). The median ADC value of lesions with underestimation was 1.26×10^{-3} mm²/sec, substantially lower than 1.35×10^{-3} mm²/sec of those without underestimation (P value = 0.094).

Conclusion: ADC values had the potential to preoperatively predict DCIS underestimation on US-guided core needle biopsy, although a large prospective series study should be conducted to confirm these results.

Index words : Breast malignancy · Underestimation · Breast core needle biopsy
Dynamic contrast enhanced magnetic resonance imaging
Diffusion-weighted magnetic resonance imaging

INTRODUCTION

The core needle biopsy is a reliable method for

diagnosing breast lesions (1–3). However, core biopsies may provide incomplete and underestimated characterization of the lesion (4). Atypical ductal hyperplasia (ADH) underestimation is defined when a lesion is diagnosed as ADH with core needle biopsy but is later found to be ductal carcinoma *in situ* (DCIS) or invasive carcinoma at surgery and DCIS underestimation is defined when a lesion is diagnosed as DCIS with core needle biopsy but is later found to be invasive carcinoma at surgery (4). Previous studies have revealed that DCIS underestimation ranged from 15% to 55.5% (1, 5–10). This high frequency of

• Received; December 24, 2012 • Revised; March 22, 2013

• Accepted; April 17, 2013

Corresponding author : Hee Jung Moon, M.D., Ph.D.

Department of Radiology, Research Institute of Radiological Science, Severance Hospital, Yonsei University College of Medicine 250 Seongsanno, Seodaemun-gu, Seoul 120-752, Korea.

Tel. 82-2-2228-7400, Fax. 82-2-393-3035

E-mail : artemis4u@yuhs.ac

underestimation may be caused by the small volume of tissue obtained with core needle biopsy, which is not sufficient to distinguish DCIS from invasive carcinoma (2). Preoperative prediction of DCIS underestimation is important for proper treatment planning including axillary staging and prognosis prediction (11). An underestimated DCIS measuring more than 2 cm in diameter may be upgraded into IIA or greater stage through surgery, while DCIS without underestimation are stage 0 regardless of their size (12).

Dynamic contrast enhanced magnetic resonance (DCE MR) imaging is one of the sensitive modalities for differentiating invasive lesions from benign lesions (13). Previous studies have reported that DCIS tends to have delayed and decreased enhancement, and longer time to peak values on DCE MR imaging compared to invasive carcinoma (11, 14, 15). This trait can be exploited to distinguish between DCIS and invasive carcinoma through DCE MR. Recent studies have shown that diffusion-weighted (DW) imaging can also be used to differentiate malignant from benign breast lesions based on low diffusivity in carcinoma due to higher cell density (16–18). Furthermore, DW imaging is useful for distinguishing DCIS from benign lesions and even discriminating between grades of DCIS (19, 20). The mean apparent diffusion coefficient (ADC) value for DCIS on ADC mapping images was higher than that of invasive cancer (18, 21).

In light of these supportive results, the aim of this study was to investigate roles of DCE MR and DW imagings in preoperative prediction of underestimation of DCIS 2 cm or more, which were detected on ultrasound (US) and underwent US guided core needle biopsy.

MATERIALS AND METHODS

Patients

Our institutional review board approved this retrospective study, and the requirement for informed consent was waived. Between July 2010 and June 2011, 98 women had US detected lesions and were diagnosed with DCIS with US-guided core needle biopsy. Thirty-six of the 98 patients who had lesions measured more than 2 cm in maximal diameter on

DCE MR were included. Lesions less than 2 cm in maximal diameter were excluded because accurate lesion identification on ADC map was difficult in some cases. Fourteen patients were later excluded from the study: 10 were excluded because of different MR protocol, 2 did not undergo breast MR, and 2 underwent breast MR at different institutions. Finally, 22 patients with b values of 0 and 600 were included in this study. The mean age of the patients was 48.1 years (range, 32–73 years).

US examination, and US guided core needle biopsy

All breast US examinations and US guided core needle biopsies were performed by 11 dedicated breast imaging radiologists with 1–17 years of experience in breast imaging with iU22 or HDI 5000 (Philips-Advanced Technology Laboratories, Bothell, WA, USA), or Logic 9 (GE Medical Systems, Milwaukee, WI, USA) and 5–12 or 7–12 MHz linear array transducers. US guided biopsy was performed for these lesions using a 14-gauge automated TSK stericut core biopsy needle (standard type with Co-axi, TSK, Japan) at least five passes.

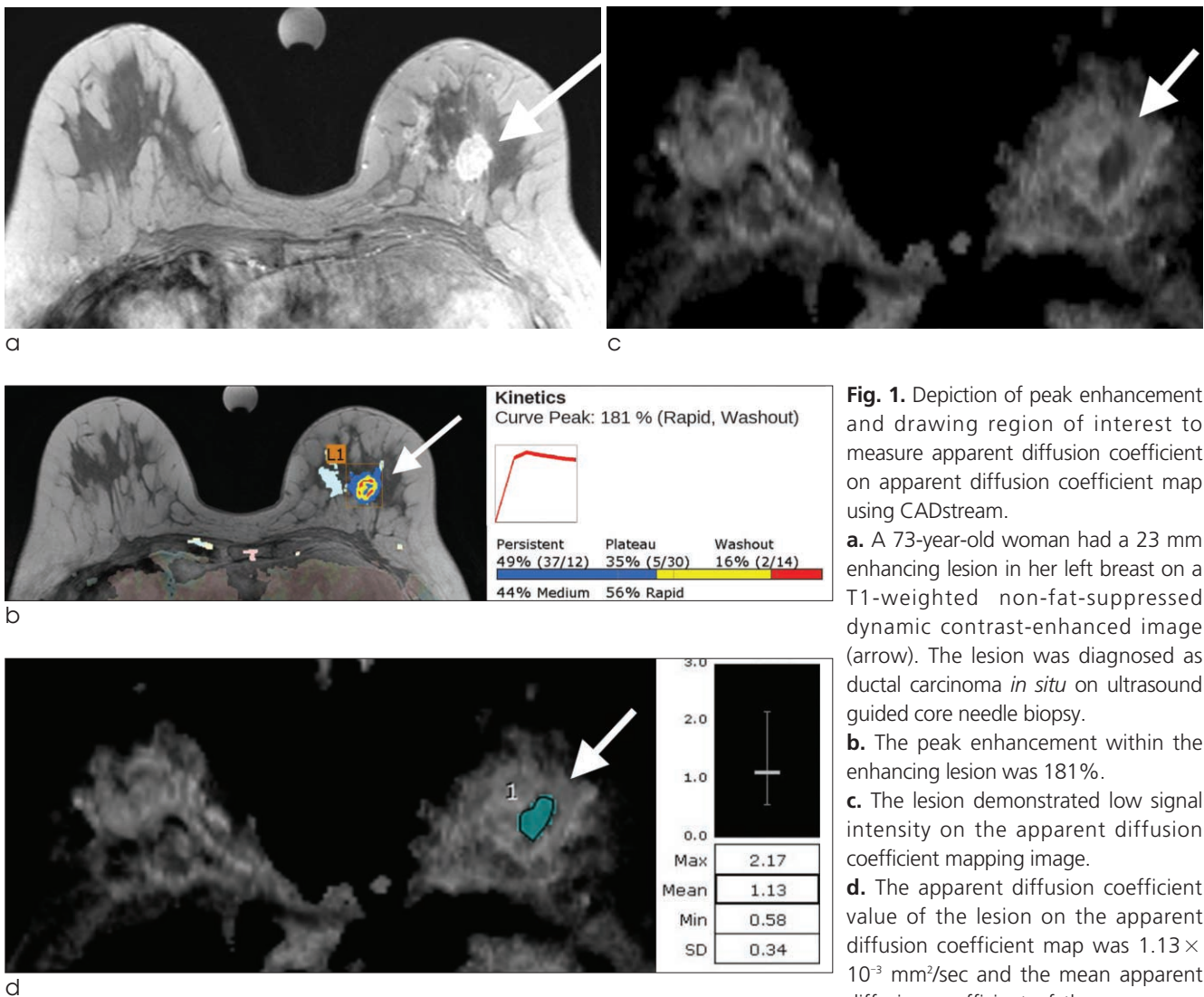
MR image acquisition and post-processing

Breast MR imaging was performed in the prone position, using a 3.0-T scanner (Trio Tim; Siemens Medical Solutions, Erlangen, Germany) equipped with a dedicated four-channel breast array coil, at least 5 days after biopsy. The following images were acquired after obtaining localizer images: T1-weighted non-fat-suppressed coronal sequence (repetition time/echo time, 280/2.6 msec; flip angle, 65°; bandwidth, 540 Hz/pixel; slice thickness, 3 mm; field of view (FOV), 340 × 340 mm; matrix size, 512 × 512; voxel size, 0.7 × 0.7 × 3.0 mm; acquisition time, 2 minutes 46 seconds), T1-weighted non-fat-suppressed axial sequence (repetition time/echo time, 280/2.6 msec; flip angle, 65°; bandwidth, 543 Hz/pixel; slice thickness, 3 mm; FOV, 340 × 340 mm; matrix size, 512 × 512; voxel size, 0.7 × 0.7 × 3.0 mm; acquisition time, 2 minutes 46 seconds), T1-weighted non-fat-suppressed pre-contrast and 2D dynamic contrast enhanced (DCE) axial (repetition time/echo time, 280/2.6 ms; flip angle, 65°; bandwidth 540 Hz/pixel; slice thickness, 3 mm; FOV, 340 × 340 mm; matrix

size, 512×343 ; voxel size, $1.0 \times 0.7 \times 3.0$ mm; acquisition time, 7 minutes 21 seconds) and coronal images (repetition time/echo time, 280/2.6 ms; flip angle, 65° ; bandwidth 540 Hz/pixel; slice thickness, 3 mm; FOV, 340×340 mm; matrix size, 512×343 ; voxel size, $0.7 \times 0.7 \times 3.0$ mm; acquisition time, 2 minutes 46 seconds), T2-weighted turbo spin echo axial images (repetition time/echo time, 4360/82 ms; flip angle, 150° ; bandwidth, 305 Hz/pixel; slice thickness, 3 mm; FOV, 360×360 mm, matrix size, 512×512 ; voxel size, $0.7 \times 0.7 \times 3.0$ mm; acquisition time, 4 minutes 23 seconds), STIR-weighted axial images (repetition time/echo time, 4400/76 ms; flip angle, 80° ; bandwidth, 303 Hz/pixel, slice thickness,

3mm; FOV, 340×340 mm, matrix size, 384×384 ; voxel size, $0.9 \times 0.9 \times 3.0$ mm; acquisition time, 3 minute 24 seconds), and DW images (repetition time/echo time, 7700/71 ms; bandwidth 1736 Hz/pixel; reduction factor, 2; number of excitations, 1; slice thickness, 3 mm; FOV, 340×340 mm; matrix size, 192×115 ; voxel size, $3.0 \times 1.8 \times 3.0$ mm; acquisition time, 3 minutes 13 seconds). DW Imaging was performed at b-values of 0 and 600.

Six series of DCE MR images with axial scans were obtained for both breasts with a time interval of 60 seconds after intravenous injection of 0.2 cc/kg gadolinium-diethylenetriaminepenta acetic acid (Gd-DTPA, Magnevist; Berlex Laboratories, Inc.,



Montville, NJ, USA). After six series of DCE MR images, delayed series of coronal sections were obtained. Pre-contrast images of the dynamic series were subtracted from the post-contrast images through post processing. Maximum intensity projection (MIP) images were acquired in axial, sagittal, and coronal planes. DW images were acquired after the DCE MR imaging acquisition using a DW echo-planar imaging (EPI) sequence with parallel imaging. ADC maps were calculated and ADC values were derived on a voxel-by-voxel basis as follows: $ADC = (1/b) \times \ln(S_0/S)$, where S_0 and S are the signal intensities of each voxel obtained with the b values of 0 and 600, respectively.

Data and statistical analysis

The standard reference was based on the histopathology of surgery. The group with underestimation was diagnosed with DCIS by US-guided core needle biopsy, and later found to have invasive cancer at breast surgery. The group without underestimation

was diagnosed with DCIS at both US guided core needle biopsy and surgery. The median age of two groups were calculated and compared using Mann whitney U test. The palpability and menopause status of two groups were compared using Fisher's exact test.

MR images including DCE MR and DW imaging were retrospectively reviewed and analyzed for this study by a radiologist with 9 years of experience in breast imaging. The radiologist was blinded to the final histopathologic results. DCE MR and DW images were analyzed with a computer aided detection system (CADstream software, version 5.2.8.591, Merge Healthcare, Milwaukee, WI, USA). The lesion size (transverse diameter, longitudinal diameter, and anterior posterior diameter) was also automatically measured on DCE MR at 2 minutes. Based on DCE MR, lesion types were classified as either a mass or a non-mass like enhancement. The enhancement pattern was automatically measured on the two minute enhancement image and classified as washout, plateau,

Table 1. Comparison of Patient Demographics and Magnetic Resonance Imaging Characteristics (dynamic contrast enhanced and diffusion-weighted) between Groups with Ductal Carcinoma *in situ* with and without Underestimation

	With underestimation (n=8)	Without underestimation (n=14)	P value
Median age (years, range)	42 (34-73)	47.5 (32-65)	0.759 #
Palpability			
Palpable (n=15)	7	8	0.193*
Non-palpable (n=7)	1	6	
Menopausal status			
Pre-menopause (n=13)	5	8	1.000*
Post-menopause (n=9)	3	6	
Median mass size on MRI (mm, range)	28.5 (20-87)	42 (20-60)	0.250#
Lesion type			
Mass (n=15)	6	9	
Non-mass (n=7)	2	5	
Enhancement pattern			
Plateau (n=5)	1	4	
Wash out (n=17)	7	10	
Median value of peak enhancement (% , range)	159.5 (76-194)	133.5 (66-233)	0.413#
Median ADC ($\times 10^{-3}$ mm ² /sec, range)	1.26 (0.96-2.15)	1.35 (1.17-1.67)	0.094#

Note.— ADC; apparent diffusion coefficient

#; Mann Whitney U test

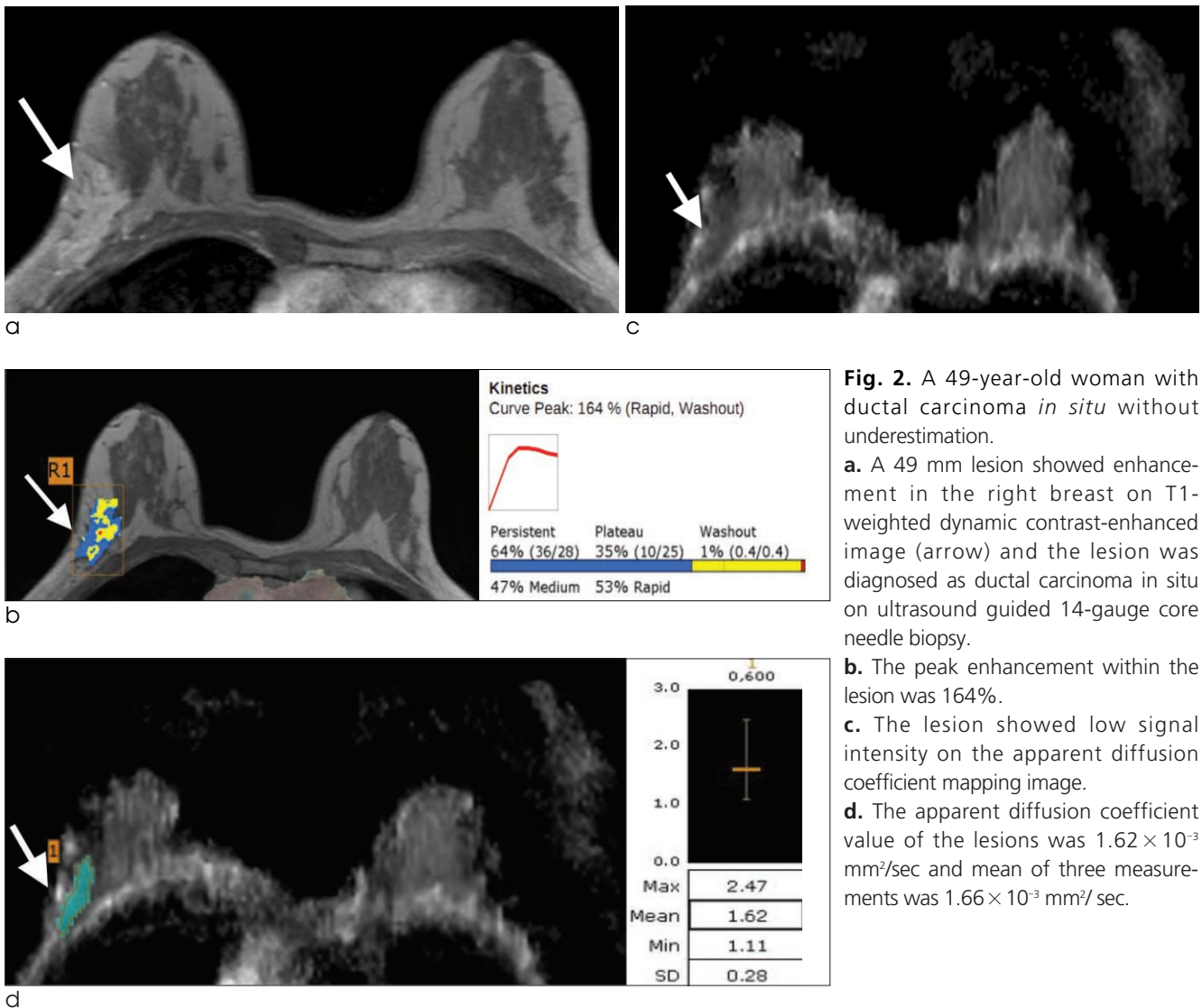
* ; Fisher's exact test

and persistent. If the signal intensity decreased by greater than 10%, then the pattern is defined as washout, and increased by greater than 10%, then the pattern is defined as persistent (22). The peak enhancement within a lesion, which was determined to be highest enhancement within the lesion based on the pre-contrast image. The enhancement pattern and peak enhancement were automatically obtained when the radiologist depicted the lesion on the CADstream software (Fig. 1a and b). The region of interest (ROI) was manually drawn on the ADC map and the ADC value of the lesion was depicted by a voxel with CADstream software (Fig. 1c and d). The radiologist chose one slice which most clearly depicted the tumor. ADC values were measured three times for the

selected image and for 2 other consecutive images, above and below. Their mean value was used for analysis. Fisher's exact test was used for comparison of lesions type and enhancement pattern and Mann Whitney test was used to compare peak enhancement and ADC values between the two groups. Two sided $p < 0.05$ was considered as statistically significant. Statistical analysis was performed with SPSS software (PASW Statistics, version 20; SPSS, Chicago, Ill.).

RESULTS

Among the 22 patients, 14 underwent total mastectomy and 8 underwent breast conserving surgery.



Eight (36.4%, 8 of 22) were confirmed to have invasive ductal carcinoma at surgery and were placed in the group with underestimation. Fourteen patients (63.6%, 14 of 22) had DCIS at surgery and were placed in the group without underestimation. In these 14 patients, 7 had high grade DCIS, 5 had intermediate grade DCIS and 2 had low grade DCIS.

The median age of the patients in the groups with and without underestimation were 42 years and 47.5 years respectively, and the difference was not significant (P value = 0.759, Table 1). The palpability and menopausal status were not different between the two groups (P values = 0.193 and 1.000, respectively).

The median size of lesions measured on DCE MR was 42 mm in the patients without underestimation (range; 20–60 mm), larger than of those with underestimation (28.5 mm, range; 20–87 mm), but the difference was not significant (P value = 0.250). The lesion type and enhancement pattern were not significantly different between two groups (P values = 1.000 and 0.613, respectively). The median peak enhancement of lesions with DCIS underestimation was 159.5%, higher than 133.5% of lesions without underestimation, but there was no statistical significance (P value = 0.413). The median ADC value of lesions with DCIS underestimation was 1.26×10^{-3} mm²/sec, lower than that of lesions without underestimation (1.35×10^{-3} mm²/sec) but not statistically significant (P value = 0.094, Figs. 1 and 2).

DISCUSSION

US-guided core needle biopsy may underestimate the invasiveness of breast cancer to DCIS or ADH or underestimate DCIS to ADH, because the core biopsy specimen only represents some part of the whole lesion (1, 2, 4, 5, 9, 19). The underestimation of our study was found in 36.4% of patients with the initial diagnosis of DCIS, which is comparable with previous studies that report underestimation in 15–55.5% of patients (1, 2, 4, 5, 19).

It is important to preoperatively determine the invasiveness of breast lesions diagnosed with core needle biopsy because axillary staging is generally not necessary for patients without DCIS underestimation but patients with DCIS underestimation may lead to a

second operation to determine axillary staging (23, 24). Invasive carcinomas more than 2 cm in diameter can be changed into stage IIA at surgery regardless of lymph node metastasis, but a DCIS of any size is stage 0 (12). The 5-year survival rate of patients with invasive tumors of stage IIA is 81%, while the patients with DCIS showed 93% survival rate (25). Thus, accurate preoperative prediction of DCIS underestimation is essential for planning treatment and estimating a prognosis (11).

Breast MR imaging is a non-invasive and highly sensitive modality for the detection of breast carcinoma and an important preoperative staging tool for patients with breast carcinoma on biopsy (26–28). As mammography cannot detect non-calcified DCIS and may underestimate the extent of disease, and US-guided core needle biopsy may underestimate the invasiveness of breast cancer, as we mentioned already, there have been studies to evaluate usefulness of breast MRI to characterize DCIS (9, 29). Some of the studies proposed that DCIS demonstrates segmental or regional distributed non-mass like enhancement, with clumped enhancement with higher ADC value than that of invasive disease which can be helpful for precise diagnosis of DCIS using breast MRI (18, 20, 29). However, none of the study have been performed to evaluate value of DCE MR and DW imaging especially in detection of DCIS underestimation, thus we evaluated usefulness of DCE MR and DW imaging in prediction of DCIS underestimation.

DCE MR imaging is used to characterize the breast lesions using the rate of contrast uptake and washout. This measure reflects the perfusion and diffusion of contrast materials into the breast lesion (30). Unlike invasive carcinoma with rapid enhancement and washout curves, DCIS tends to show delayed and decreased enhancement (30, 31). The kinetic curve of invasive carcinoma of fast contrast material uptake and a rapid washout is more accentuated when the invasive carcinoma extends to a axillary lymph node (11). The kinetic pattern can predict the invasiveness of breast carcinoma as well as lymph node metastasis (11). For kinetic pattern analysis, we used CADstream software because previous studies showed that CAD-based analysis improved the discrimination of benign from malignant breast lesions at MRI by providing more objective and detailed information (32, 33).

Furthermore, different enhancement pattern in delayed enhancement between DCIS and invasive carcinoma was also observed in the study using CADstream software (34). In our study, patients with DCIS underestimation showed higher peak enhancement percentages compared to those without (159.5% vs. 133.5%) though the difference was not statistically significant (P value = 0.413). Although the results of our study did not show statistical significance due to limited sample size, they were consistent with the hypothesis that kinetic curve may reflect the invasiveness of the lesion (11, 35). In this study, we also analyzed lesion type according to the mass like or non-mass like enhancement on DCE MR and there was no significant difference between the group with or without underestimation (P value = 1.000). This may account for inclusion criteria of the study, which only included the lesions detectable on US, thus non-mass like enhancement lesion has a potential to be missed on US (31, 36).

DW imaging also reflects the tissue cellularity and helps differentiate malignant lesions from benign ones (18–21, 37, 38). ADC values show negative correlation with cellular density, thus highly cellular lesions, such as invasive carcinoma, have lower ADC values than DCIS (18–21, 37, 38). The association between ADC value and DCIS grade shows negative correlation (19). The ADC value of 1.3×10^{-3} mm²/sec is determined as the cut-off for distinguishing low grade DCIS from intermediate and high grade DCIS (19). ADC values of DCIS are ranging from 1.12×10^{-3} mm²/sec to 1.5×10^{-3} mm²/sec, but ADC values of invasive disease ranged between 0.92×10^{-3} mm²/sec to 1.22×10^{-3} mm²/sec, lower than that of DCIS (18, 20, 39). In our study, DCIS with underestimation had lower ADC values than those without underestimation (median ADC: 1.26×10^{-3} mm²/sec and 1.35×10^{-3} mm²/sec, respectively, P = 0.094). ADC values had the potential to preoperatively differentiate DCIS with underestimation from DCIS without underestimation. Although ADC values are different in each institution because of the different MR scanners and protocols, ADC value can differentiate the malignant and benign lesions and discriminate the grade of DCIS (18–20, 39, 40).

This study had several limitations. First, DW imaging was performed after DCE MR imaging in our study.

Contrast material decreases the ADC values though there is not statistical significance in some studies (37). The purpose of our study was to compare the ADC values of DCIS with or without underestimation and so this MR protocol did not impact the result of our study. Second, we included only DCIS diagnosed with US guided core needle biopsy. DCIS with microcalcifications only found on mammography underwent stereotactic biopsy. Stereotactic biopsies were performed at our institution using a vacuum-assisted device with 8 or 11 gauge needles, and were, therefore, not included. Third, a single reader evaluated ADC values with manually drawn ROIs on ADC maps and intra-observer variability was not assessed, although the mean ADC value was used after three measurements. Fourth, MR imaging was performed at least 5 days after biopsy in our study. This may cause post-biopsy changes such as hemorrhage and fluid collection, even it is infrequent on MR imaging as reported as 3% (41). In our study, the ADC value was obtained at solid mass excluding gross hemorrhage if existed, however hemorrhage which was not visualized in the ADC map might impact the ADC value. Fifth, this study included a small number of patients and the results were not statistically significant. A large-scale prospective study is needed to verify our findings.

In conclusion, ADC values had the potential to preoperatively predict underestimation of DCIS on US-guided core needle biopsy, although a large prospective series study should be conducted to confirm these results.

References

- Schuelter G, Jaromi S, Ponhold L, et al. US-guided 14-gauge core-needle breast biopsy: results of a validation study in 1352 cases. *Radiology* 2008;248:406
- Liberman L. Clinical management issues in percutaneous core breast biopsy. *Radiol Clin North Am* 2000;38:791-807
- Youk JH, Kim EK, Kwak JY, Son EJ, Park BW, Kim SI. Benign papilloma without atypia diagnosed at US-guided 14-gauge core-needle biopsy: clinical and US features predictive of upgrade to malignancy. *Radiology* 2011;258:81-88
- O'Flynn EA, Wilson AR, Michell MJ. Image-guided breast biopsy: state-of-the-art. *Clin Radiol* 2010;65:259-270
- Helbich TH, Matzek W, Fuchsjäger MH. Stereotactic and ultrasound-guided breast biopsy. *Eur Radiol* 2004;14:383-393
- Sauer G, Deissler H, Strunz K, et al. Ultrasound-guided large-core needle biopsies of breast lesions: analysis of 962 cases to

- determine the number of samples for reliable tumour classification. *Br J Cancer* 2004;92:231-235
7. Schoonjans JM, Brem RF. Fourteen-gauge ultrasonographically guided large-core needle biopsy of breast masses. *J Ultrasound Med* 2001;20:967-972
 8. Smith DN, Rosenfield Darling ML, Meyer JE, et al. The utility of ultrasonographically guided large-core needle biopsy: results from 500 consecutive breast biopsies. *J Ultrasound Med* 2001;20:43-49
 9. Suh Y, Kim M, Kim E, et al. Comparison of the underestimation rate in cases with ductal carcinoma in situ at ultrasound-guided core biopsy: 14-gauge automated core-needle biopsy vs 8-or 11-gauge vacuum-assisted biopsy. *Br J Radiol* 2012;85:e349-e356
 10. Verkooijen HM, Peeters PH, Buskens E, et al. Diagnostic accuracy of large-core needle biopsy for nonpalpable breast disease: a meta-analysis. *Br J Cancer* 2000;82:1017-1021
 11. Bhooshan N, Giger ML, Jansen SA, Li H, Lan L, Newstead GM. Cancerous breast lesions on dynamic contrast-enhanced MR images: computerized characterization for image-based prognostic markers. *Radiology* 2010;254:680-690
 12. Edge SB, Byrd DR, Compton CC, Fritz AG, Greene FL, Trotti A. *AJCC Cancer Staging Manual*. 7th ed. Chicago, IL: Springer, 2009.
 13. Kuhl CK, Schild HH. Dynamic image interpretation of MRI of the breast. *J Magn Reson Imaging* 2000;12:965-974
 14. Van Goethem M, Schelfout K, Kersschot E, et al. Comparison of MRI features of different grades of DCIS and invasive carcinoma of the breast. *JBR BTR* 2005;88:225-232
 15. Chen W, Giger ML, Li H, Bick U, Newstead GM. Volumetric texture analysis of breast lesions on contrast-enhanced magnetic resonance images. *Magn Reson Med* 2007;58:562-571
 16. Peters NH, Vincken KL, van den Bosch MA, Luijten PR, Mali WP, Bartels LW. Quantitative diffusion weighted imaging for differentiation of benign and malignant breast lesions: the influence of the choice of b-values. *J Magn Reson Imaging* 2010;31:1100-1105
 17. Rubesova E, Grell AS, De Maertelaer V, Metens T, Chao SL, Lemort M. Quantitative diffusion imaging in breast cancer: a clinical prospective study. *J Magn Reson Imaging* 2006;24:319-324
 18. Woodhams R, Matsunaga K, Kan S, et al. ADC mapping of benign and malignant breast tumors. *Magn Reson Med Sci* 2005;4:35-42
 19. Iima M, Le Bihan D, Okumura R, et al. Apparent diffusion coefficient as an MR imaging biomarker of low-risk ductal carcinoma in situ: a pilot study. *Radiology* 2011;260:364-372
 20. Rahbar H, Partridge SC, Eby PR, et al. Characterization of ductal carcinoma in situ on diffusion-weighted breast MRI. *Eur Radiol* 2011;21:2011-2019
 21. Partridge SC, Demartini WB, Kurland BF, Eby PR, White SW, Lehman CD. Differential diagnosis of mammographically and clinically occult breast lesions on diffusion-weighted MRI. *J Magn Reson Imaging* 2010;31:562-570
 22. Moon M, Cornfeld D, Weinreb J. Dynamic contrast-enhanced breast MR imaging. *Magn Reson Imaging Clin N Am* 2009;17:351-362
 23. Cho N, Moon WK, Chang JM, et al. Sonoelastographic lesion stiffness: preoperative predictor of the presence of an invasive focus in nonpalpable DCIS diagnosed at US-guided needle biopsy. *Eur Radiol* 2011;21:1618-1627
 24. Lyman GH, Giuliano AE, Somerfield MR, et al. American Society of Clinical Oncology guideline recommendations for sentinel lymph node biopsy in early-stage breast cancer. *J Clin Oncol* 2005;23:7703-7720
 25. Society AC. Breast cancer survival rates by stage. 2012
 26. Gutierrez RL, DeMartini WB, Silbergeld JJ, et al. High cancer yield and positive predictive value: outcomes at a center routinely using preoperative breast MRI for staging. *AJR Am J Roentgenol* 2011;196:W93-W99
 27. Houssami N, Ciatto S, Macaskill P, et al. Accuracy and surgical impact of magnetic resonance imaging in breast cancer staging: systematic review and meta-analysis in detection of multifocal and multicentric cancer. *J Clin Oncol* 2008;26:3248-3258
 28. Pengel KE, Loo CE, Teertstra HJ, et al. The impact of preoperative MRI on breast-conserving surgery of invasive cancer: a comparative cohort study. *Breast Cancer Res Treat* 2009;116:161-169
 29. Rosen EL, Smith-Foley SA, DeMartini WB, Eby PR, Peacock S, Lehman CD. BI-RADS MRI Enhancement characteristics of ductal carcinoma in situ. *Breast J* 2007;13:545-550
 30. Jansen SA. Ductal carcinoma in situ: detection, diagnosis, and characterization with magnetic resonance imaging. *Semin Ultrasound CT MR* 2011;32:306-318
 31. Sakamoto N, Tozaki M, Higa K, et al. Categorization of non-mass-like breast lesions detected by MRI. *Breast Cancer* 2008;15:241-246
 32. Lehman CD, Peacock S, DeMartini WB, Chen X. A new automated software system to evaluate breast MR examinations: improved specificity without decreased sensitivity. *AJR Am J Roentgenol* 2006;187:51-56
 33. Meeuwis C, Van de Ven SM, Stapper G, et al. Computer-aided detection (CAD) for breast MRI: evaluation of efficacy at 3.0 T. *Eur Radiol* 2010;20:522-528
 34. Wang LC, DeMartini WB, Partridge SC, Peacock S, Lehman CD. MRI-detected suspicious breast lesions: predictive values of kinetic features measured by computer-aided evaluation. *AJR Am J Roentgenol* 2009;193:826-831
 35. Jansen SA, Newstead GM, Abe H, Shimauchi A, Schmidt RA, Karczmar GS. Pure ductal carcinoma in situ: kinetic and morphologic MR characteristics compared with mammographic appearance and nuclear grade. *Radiology* 2007;245:684-691
 36. Newell D, Nie K, Chen JH, et al. Selection of diagnostic features on breast MRI to differentiate between malignant and benign lesions using computer-aided diagnosis: differences in lesions presenting as mass and non-mass-like enhancement. *Eur Radiol* 2010;20:771-781
 37. Woodhams R, Ramadan S, Stanwell P, et al. Diffusion-weighted imaging of the breast: principles and clinical applications. *Radiographics* 2011;31:1059-1084
 38. Kuroki-Suzuki S, Kuroki Y, Nasu K, Nawano S, Moriyma N, Okazaki M. Detecting breast cancer with non-contrast MR imaging: combining diffusion-weighted and STIR imaging. *Magn Reson Med Sci* 2007;6:21-27
 39. Marini C, Iacconi C, Giannelli M, Cilotti A, Moretti M, Bartolozzi C. Quantitative diffusion-weighted MR imaging in the differential diagnosis of breast lesion. *Eur Radiol* 2007;17:2646-2655
 40. Kuhl CK, Schrading S, Bieling HB, et al. MRI for diagnosis of pure ductal carcinoma in situ: a prospective observational study. *Lancet* 2007;370:485-492

41. Liberman L, Morris EA, Dershaw DD, Abramson AF, Tan LK.
MR imaging of the ipsilateral breast in women with percuta-

neously proven breast cancer. AJR Am J Roentgenol
2003;180:901-910

대한자기공명의과학회지 17:101-109(2013)

역동적 유방 자기공명 영상 및 확산 강조영상을 이용한 관상피내암종 저평가 수술전 예측

연세대학교 의과대학 세브란스병원 영상의학과

박미나 · 김은경 · 김민정 · 문희정

목적: 초음파 유도 하 중심부 침생검으로 진단된 2 cm 이상의 관상피내암종 저평가 수술 전 예측에 역동적 유방 자기공명 영상 및 확산강조영상의 역할을 규명하고자 한다.

대상과 방법: 14 gauge침을 이용한 초음파 유도 하 중심부 침생검을 통해 관상피내암종으로 진단된 22명의 환자를 대상으로 하였다. 환자는 조직병리 결과에 의거하여 관상피내암종 저평가 유무에 따라 두 군으로 나뉘었다. 모든 환자에서 역동적 유방 자기공명 영상 및 확산강조영상을 포함한 3 테슬라 유방 자기공명 영상을 획득하였다. 생검으로 확인된 악성 종괴에 대해, 병변의 형태 (종괴 혹은 비종괴), 조영 증강 형태, 조영 증강 최고점, 및 현성 확산 계수를 CADstream 소프트웨어를 이용하여 획득 하였으며, Fisher's exact test 및 Mann Whitney test 이용하여 이 항목을 비교, 분석하였다.

결과: 총 22명의 환자 중 8명의 환자가 저평가 군으로 분류되었다. 병변의 형태 및 조영증강 형태는 두 군의 통계학적 차이가 없었다 (P values = 1.000 및 0.613). 조영 증강 최고점의 중앙값은 저평가 군에서 159.5% 로 저평가 되지 않은 군의 133.5% 보다 높았으나 통계학적 유의한 차이를 보이지 않았다 (P value = 0.413). 저평가 군의 현성 확산 계수는 $1.26 \times 10^{-3} \text{ mm}^2/\text{sec}$ 로 저평가 되지 않은 군의 $1.35 \times 10^{-3} \text{ mm}^2/\text{sec}$ 보다 낮았다 (P value = 0.094).

결론: 현성 확산 계수는 초음파 유도한 중심부 침생검에 의한 관상피내암종 저평가 수술 전 예측에 도움이 될 가능성이 있으며 추후 전향적 연구를 통해 이 연구 결과를 확인하는 것이 필요하겠다.

통신저자 : 문희정, (120-752) 서울시 서대문구 연세로 50, 세브란스병원 영상의학과
Tel. (02) 2228-7400 Fax. (02) 393-3035 E-mail: artemis4u@yuhs.ac